Korean J. Chem. Eng., **29**(3), 310-316 (2012)
DOI: 10.1007/s11814-011-0171-9

Preparation of CoMoS catalysts for hydrodesulfurization using methylacetoacetate as a chelating agent

Sang Il Lee*,, Ara Cho*, Jae Hyun Koh**, and Sang Heup Moon*,†**

*School of Chemical & Biological Engineering and Institute of Chemical Processes, Seoul National University, Seoul 151-744, Korea
**Institute of Technology, SK Innovation Co., Ltd., Daejeon 305-712, Korea
(*Received 31 May 2011 • accepted 5 July 2011*)

Abstract–$CoMoS/Al_2O_3$ catalyst, which was prepared using $Co(MeAA)_2 \cdot 2H_2O$ as a new Co precursor, showed activity for hydrodesulfurization (HDS) higher than that of conventional catalysts, which were prepared using $Co(NO_3) \cdot 6H_2O$ as a Co precursor and/or by adding ethylene-di-amine-tetra-acetic acid (EDTA) as a chelating agent. Catalyst of a similar activity was also obtained simply by impregnating a conventional $CoMo/Al_2O_3$ catalyst with an aqueous solution of methylacetoacetate (MeAA) followed by drying and sulfidation. The added MeAA reacted with Co to produce $Co(MeAA)_2 \cdot 2H_2O$ on the catalyst surface during impregnation step, such that the resulting catalyst became similar to one prepared by direct impregnation with $Co(MeAA)_2 \cdot 2H_2O$. The *in-situ* synthesis of $Co(MeAA)_2 \cdot 2H_2O$ on the catalyst surface was advantageous over the method of directly adding the Co precursor to the impregnation solution because the former method did not use a basic material, which was required for the synthesis of the Co precursor. Furthermore, MeAA was soluble in water, whereas $Co(MeAA)_2 \cdot 2H_2O$ had to be dissolved in an organic solvent, e.g., 1,4-dioxane. The Co species in the MeAA-added catalysts were sulfided at temperatures higher than those of conventional catalysts, and consequently the former catalysts contained greater amounts of the HDS-active CoMoS phase than the latter.

Key words: Hydrodesulfurization, CoMoS, Methylacetoacetate, Chelating Agent

INTRODUCTION

Improvement in the activity of current hydrotreating catalysts is required to meet recent stringent environmental regulations demanded for low sulfur contents of transportation fuels [1,2]. The majority of commercial hydrotreating catalysts are composed of Co (or Ni) and Mo dispersed on supports [3-6]. The HDS-active center is the so-called "CoMoS (or NiMoS) phase," which consists of sulfided Co or Ni atoms on the edges and corners of MoS_2 crystallites [4,6-8]. Numerous studies have been made to prepare catalysts containing increased amounts of the active CoMoS or NiMoS phase.

Organic chelating agents, such as nitrilotriactic acid (NTA), citric acid (CA), ethylene-di-amine-tetra-acetic acid (EDTA) and their derivatives, have been widely used in the preparation of HDS catalysts because they promote the formation of the CoMoS phase during catalyst sulfidation [9-13]. The mechanism of catalyst promotion by the chelating agent was investigated previously. Kubota et al. reported, based on their study of CA-added catalysts, that added CA suppressed the sulfidation of Co such that Mo component in the catalyst was sulfided prior to or in parallel with the sulfidation of Co, which produced increased amounts of the CoMoS phase [10]. Shimizu et al. studied the effect of chelating agents, e.g., NTA, EDTA and *trans*-1,2-cyclohexanediamine-N,N,N′,N′-tetraacetic acid (CyDTA), on the performance of various catalysts, e.g., CoMo, NiMo and NiW. They reported that the beneficial effect of chelating agents originated from the stability of a promoter-chelating agent complex that eventually allowed the formation of highly active sites [13].

On the other hand, Frizi et al. observed that the length of MoS_2 slabs increased due to the retarded migration of Co on the MoS_2 edge when the stability of the Co-chelating agent complex was excessive as in the case of Co(EDTA) [14,15]. They also proposed that the simultaneous sulfidation of Mo and Co was responsible for a decrease in the MoS_2 slab length and an increase in the number of Co atoms that decorated the Mo sites.

In this study, we used cobalt methylacetoacetate, $Co(MeAA)_2 \cdot 2H_2O$ as a new Co precursor to take advantage of its moderate stability compared with a Co-EDTA complex. We also attempted to find a new method for modifying the Mo surface with $Co(MeAA)_2 \cdot 2H_2O$ by producing the latter *in situ* on the catalyst surface instead of by directly adding the Co precursor to impregnation solution. The HDS activity of prepared catalyst was measured using dibenzothiophene (DBT) and 4,6-dimethyldibenzothiophene (4,6-DMDBT) as model reactants. The catalyst surface was characterized using Fourier transform infrared (FTIR) spectroscopy, temperature-programmed sulfidation (TPS), temperature-programmed reduction (TPR) and high-resolution transmission electron microscopy (HRTEM).

EXPERIMENTAL

1. Catalyst Preparation

$Co(MeAA)_2 \cdot 2H_2O$ was synthesized by a known method [16]: 10 g of MeAA was added to a solution, containing 3.5 g of NaOH and 153 g of methanol, with stirring. The MeAA-containing solution was added drop-wise to a solution containing 10.3 g of cobalt(II) chloride hexa-hydrate in 161 g of methanol with vigorous stirring.

†To whom correspondence should be addressed.
E-mail: shmoon@surf.snu.ac.kr

The resulting pale-pink precipitates, $Co(MeAA)_2 \cdot 2H_2O$, were filtered and washed with 500 g of methanol. To purify the crude $Co(MeAA)_2 \cdot 2H_2O$, the precipitates were dissolved in 100 g of 1,4-dioxane and filtered. Then, 400 g of methanol was added to the filtered 1,4-dioxane solution to make pure precipitates. Finally, the precipitates were filtered, washed with 300 g of methanol and dried at 353 K for two days at a pressure of 50 mbar.

$Co(MeAA)_2$-impregnated catalyst was prepared by sequentially loading γ-Al_2O_3 with Mo and Co. That is, 30 g of γ-Al_2O_3 was impregnated with 10.8 g of $(NH_4)_6Mo_7O_{24} \cdot 4H_2O$ in aqueous solution, followed by drying in air at 393 K for 2 h (designated as Mo(d)) and final calcination in air at 773 K for 2 h (designated as Mo(c)). Mo(c) was additionally impregnated with $Co(MeAA)_2 \cdot 2H_2O$ dissolved in 1,4-dioxane, followed by drying in air at 473 K for 2 h (designated as Co(M)Mo(c)).

Two types of catalysts were prepared using $Co(NO_3)_2 \cdot 6H_2O$ as a Co precursor. Mo(c) was impregnated with $Co(NO_3)_2 \cdot 6H_2O$ in aqueous solution, followed by drying in air at 393 K for 2 h (designated as Co(d)Mo(c)) and final calcination in air at 773 K for 2 h (designated as Co(c)Mo(c)).

The two catalysts, Co(d)Mo(c) and Co(c)Mo(c), were additionally impregnated with an increasing amount of MeAA, which was dissolved in an aqueous solution, followed by drying in air at 473 K for 2 h (designated as Co(d)Mo(c)_xM and Co(c)Mo(c)_xM, x being the mole ratio of MeAA/Co).

To compare the effect of MeAA with that of EDTA, a known chelating agent in commercial use, a series of EDTA-containing catalysts were prepared as reported previously [17]. Mo(d) or Mo(c) was impregnated with $Co(NO_3)_2 \cdot 6H_2O$ and EDTA, which was dissolved in an NH_4OH-added aqueous solution, followed by drying in air at 393 K for 3 h. The catalysts were designated as Co(E)Mo(c) and Co(E)Mo(d) according to the post-treatment conditions of Mo/Al_2O_3. The mole ratio of EDTA/Co was 1.2. The nominal contents of Co and Mo in all catalysts were 4 wt% and 15 wt%, respectively.

Two sample catalysts were prepared for TPS experiments by impregnating γ-Al_2O_3 with $Co(NO_3)_2 \cdot 6H_2O$ and subsequently with or without MeAA. That is, $Co(NO_3)_2/Al_2O_3$ with a Co content of 4 wt% was prepared by impregnating γ-Al_2O_3 with $Co(NO_3)_2 \cdot 6H_2O$ in aqueous solution, followed by drying in air at 473 K for 2 h (designated as Co(d)). The other sample, Co(d)_M, was prepared by adding MeAA to Co(d), followed by drying in air at 473 K for 2 h.

2. Reaction

Prior to use in HDS, all CoMo catalysts were pre-sulfided in a pentadecane solution containing 30 vol% of dimethyldisulfide (DMDS) at 623 K under a hydrogen pressure of 4.0 MPa for 4 h. Mo(c) was sulfided at a temperature of 673 K. After sulfidation, the catalysts were used for the HDS of DBT or 4,6-DMDBT in an autoclave at 593 K under a hydrogen pressure of 4.0 MPa. The reactor contained 0.03 g of DBT or 4,6-DMDBT dissolved in 30 cm^3 of pentadecane or dodecane, respectively. The amounts of catalysts charged in the reactor were 0.05 g for the HDS of DBT and 0.1 g for the HDS of 4,6-DMDBT. Reaction products were analyzed with a gas chromatograph (HP5890, Agilent) equipped with a flame ionization detector and a silicone capillary column.

3. Characterization

IR spectra of catalysts or gases adsorbed on the catalysts were recorded by using a Nicolet 6700 model FT-IR spectrometer at a resolution of 4 cm^{-1} and 200 scans per spectrum. To analyze possible changes in the property of MeAA during catalyst preparation, a self-supporting wafer (10-15 mg/cm^2) of catalysts, either containing MeAA or not and either dried or calcined after cobalt introduction, was prepared by pressing the catalyst powders. The wafer was placed in an IR cell, heated to 573 K, and maintained at the temperature in Ar flow for 1 h, followed by cooling to 313 K. The IR spectrum of the wafer was recorded at 313 K after the cell was degassed at pressures below 10^{-3} mbar.

To obtain IR spectra of NO adsorbed on the catalysts, a self-supporting wafer of sulfided catalyst was introduced into an IR cell, heated to 573 K, and maintained at a constant temperature in a flow of 10% H_2/N_2 for 2 h. The flowing gas was switched to Ar and the temperature was maintained at 573 K for 0.5 h, after which the cell was cooled to 313 K. An IR spectrum was recorded at 313 K after the cell was degassed at 10^{-3} mbar. The spectrum was measured again after the catalyst was exposed to 15 Torr of NO for 5 min, followed by degassing of the cell. The IR spectrum of adsorbed NO was obtained from the difference between the above two measurements.

TPR experiments were performed using an Autochem II model of Micromeritics equipped with a thermal conductivity detector (TCD) and a low temperature trap for the removal of desorbed water during the experiments. Sulfided samples, obtained under the condition described above (section 2.2), were treated in a flow of N_2 at 473 K for 1 h, cooled to room temperature, and finally heated to 750 K at a rate of 5 K/min in a flowing gas mixture of 5 vol% H_2/N_2. The signal of H_2 consumption was measured by a TCD.

TPS was performed in a reactor connected with a mass spectrometer. Samples were treated in a flow of N_2 at 473 K for 1 h, cooled to room temperature, and finally heated to 773 K at a rate of 5 K/min in a flow mixture of 10 vol% H_2S/H_2. The H_2S signal was measured by mass spectroscopy.

HRTEM was obtained using Tecnai^{TM} G^2 F30 operated at 300 kV. Samples were ground in a mortar and dispersed in heptanes. A drop of suspension liquid was placed on a micro holy grid. To estimate the average length and stacking degree of MoS_2 slabs, more

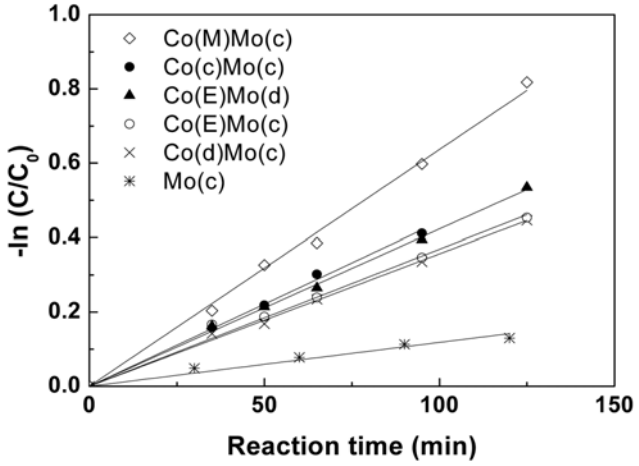

Fig. 1. HDS of DBT on MoS_2/Al_2O_3 and $CoMoS/Al_2O_3$ catalysts prepared from different cobalt precursors. Sample notations are described in section 2.1.

than 200 crystallites were measured.

RESULTS

1. HDS of DBT and 4,6-DMDBT

Fig. 1 shows plots of DBT conversions obtained using six different catalysts, assuming that the reaction followed first-order kinetics. The activity increased in an order, Mo(c)<<Co(d)Mo(c)~Co(E)Mo(c)<Co(E)Mo(d)<Co(c)Mo(c)<Co(M)Mo(c), demonstrating the promotional effect of Co and the advantage of $Co(MeAA)_2 \cdot 2H_2O$ as a Co precursor. It is noteworthy that Co(M)Mo(c) showed the highest activity among sample catalysts, i.e., higher than those prepared using $Co(NO_3)_2 \cdot 6H_2O$ as a Co precursor, Co(d)Mo(c) and Co(c)Mo(c), or using EDTA as a chelating agent, Co(E)Mo(c) and Co(E)Mo(d). All catalysts were pre-sulfided under an identical condition, described in section 2.2, prior to use in the HDS.

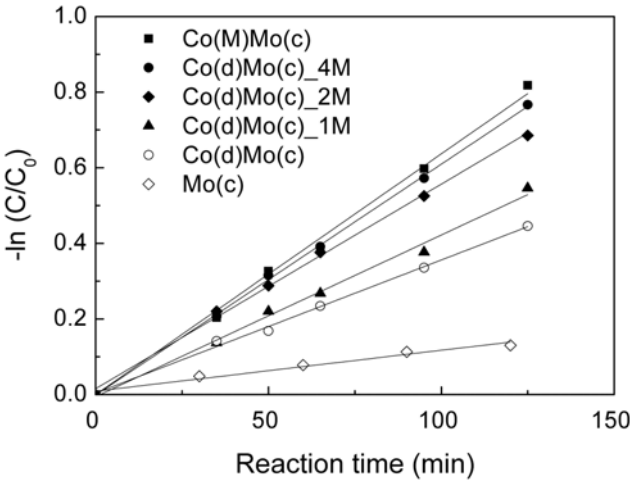

Fig. 2. HDS of DBT on MoS_2/Al_2O_3 and $CoMoS/Al_2O_3$ catalysts prepared by adding different amounts of MeAA. Sample notations are described in section 2.1.

Table 1. Rate constants in the HDS of DBT and 4,6-DMDBT

Rate constant, k[a] (10^{-3} min^{-1}) (relative value)					
Catalyst[b]	Reaction	Mole ratio of MeAA/Co			
		0	1	2	4
Co(d)Mo(c)_xM	DBT HDS	3.6 (1.0)	4.2 (1.2)	5.6 (1.6)	6.1 (1.7)
	4,6-DMDBT HDS	3.2 (1.0)		3.9 (1.2)	
		[0.20][c]		[0.24][c]	
Co(M)Mo(c)	DBT HDS			6.3	
Co(c)Mo(c)_xM	DBT HDS	4.4 (1.0)		4.6 (1.0)	

[a]First-order reaction model was used to calculate the rate constant
[b]The amounts of catalysts were 0.05 g for DBT HDS and 0.1 g for 4,6-DMDBT HDS
[c]The ratio of DMBP to (MCHT+DMDCH) among products of 4,6-DMDBT HDS at a conversion of 40%

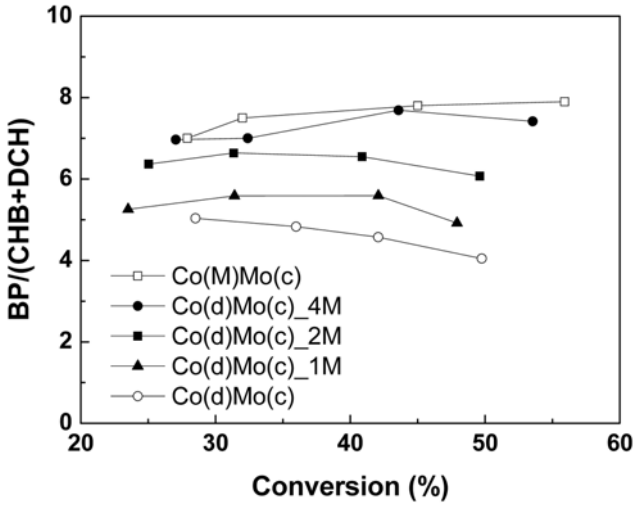

Fig. 3. Product distribution in the HDS of DBT obtained using Co MoS/Al_2O_3 catalysts prepared by adding different amounts of MeAA. Sample notations are described in section 2.1.

Fig. 2 shows the reaction results of catalysts prepared by impregnating Co(d)Mo(c) with different amounts of MeAA. The estimated rate constants are listed in Table 1. The activity of Co(d)Mo(c) increased with the amounts of added MeAA, although the increase rate became smaller at high MeAA/Co mole ratios. Eventually, the activity of Co(d)Mo(c)_4M became comparable to that of Co(M)Mo(c), which was prepared by directly adding $Co(MeAA)_2 \cdot 2H_2O$ to the preparation solution. The same trend was observed when the catalysts were used in the HDS of 4,6-DMDBT, although the activity increase was smaller than in DBT HDS. Contrary to the above results, catalysts prepared by impregnating Co(c)Mo(c) with MeAA did not show an increase in the activity, as shown for Co(c)Mo(c)_xM in Table 1. This discrepancy will be discussed in section 4.2.

The product distribution of DBT HDS was also affected by the addition of MeAA, as shown in Fig. 3. The major products were biphenyl (BP), cyclohexylbenzene (CHB) and dicyclohexyl (DCH), which could be classified into two groups, BP and CHB+DCH, according to the extent of ring saturation. BP was obtained largely by the direct desulfurization (DDS) of DBT without ring saturation, whereas CHB and DCH were obtained by the hydrogenation (HYD) of the aromatic ring [18-20]. The BP/(CHB+DCH) ratios of the MeAA-containing catalysts, Co(d)Mo(c)_xM, were higher than that of Co(d)Mo(c) and increased with the amount of added MeAA eventually to approach one for Co(M)Mo(c). The same trend was observed in the HDS of 4,6-DMDBT (Table 1) although the product distribution was obtained only for two catalysts, Co(d)Mo(c) and Co(d)Mo(c)_2M.

2. HRTEM and FTIR

Fig. 4 shows HRTEM images of three catalysts prepared using different Co precursors. The average lengths and stacking degrees of MoS_2 slabs estimated from the images are summarized in Table 2. The stacking degree of MoS_2 slabs remained nearly constant but the slab length was affected by the Co precursors. Among three sample catalysts, Co(M)Mo(c) showed the shortest slab length, i.e., the highest dispersion of MoS_2 slabs.

FTIR spectra of Co(M)Mo(c) and Co(d)Mo(c)_xM, which con-

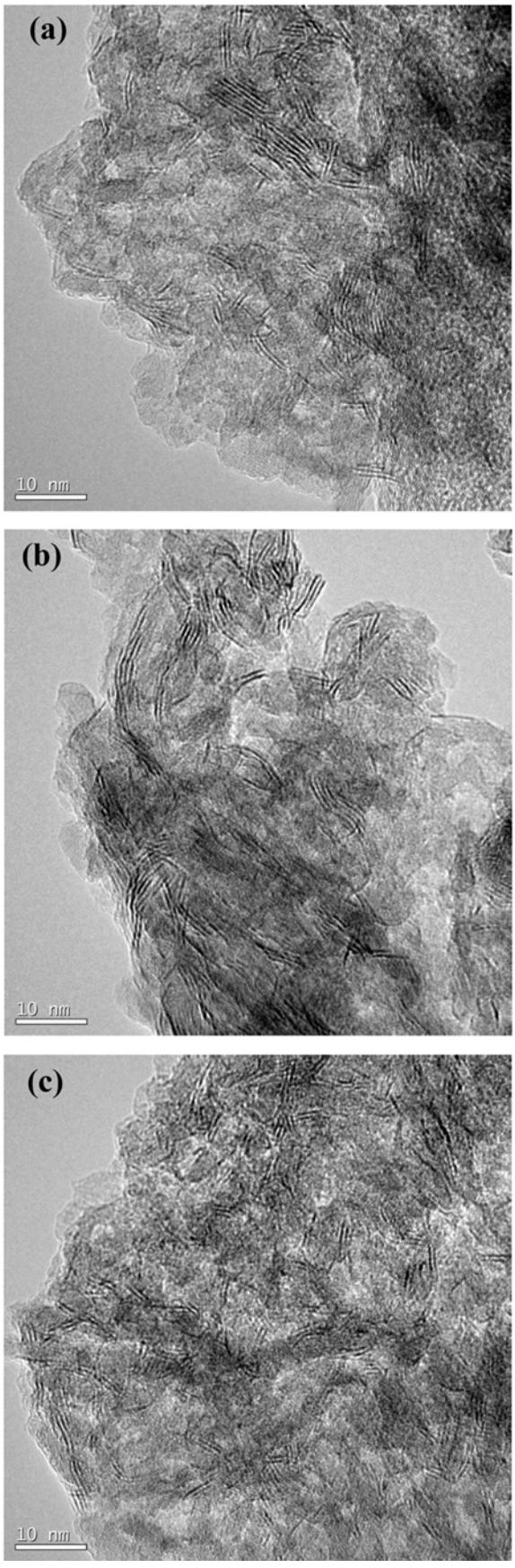

Fig. 4. HRTEM images of CoMoS catalysts: (a) Co(d)Mo(c); (b) Co(E)Mo(c); (c) Co(M)Mo(c).

Table 2. Lengths and stacking degrees of MoS_2 slabs estimated from HRTEM results (Fig. 4)

Catalysts	Co(d)Mo(c)	Co(E)Mo(c)	Co(M)Mo(c)
Average length (nm)	5.1	4.5	3.1
Average stacking degree	2.3	2.2	2.2

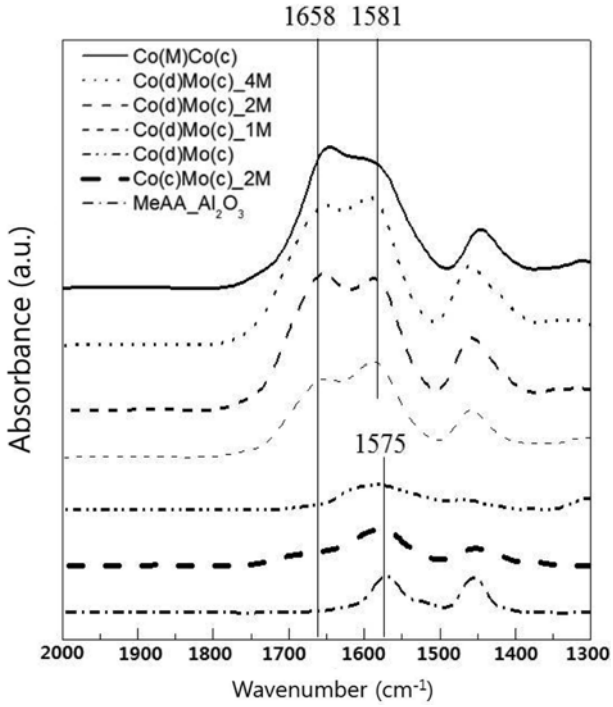

Fig. 5. FT-IR absorbance spectra of various oxidic $CoMo/Al_2O_3$ catalysts. Sample notations are described in section 2.1.

tained different amounts of MeAA, are given in Fig. 5. As the catalysts were not pre-sulfided prior to the spectral observations, they are supposed to contain oxidic species originating from metal precursors. Spectra of Co(c)Mo(c)_2M and $MeAA/Al_2O_3$ are also included for comparison. Co(M)Mo(c) showed two strong peaks at above 1,500 cm^{-1}, representing C=O and C=C groups that constituted the structure of $Co(MeAA)_2 \cdot 2H_2O$. Similar peaks were observed with Co(d)Mo(c)_xM, but in this case the peak intensity increased with the amounts of added MeAA, which suggested that $Co(MeAA)_2$ was produced by reaction between added MeAA and Co in the catalyst. Contrary to the above, Co(d)Mo(c), Co(c)Mo(c)_2M and $MeAA/Al_2O_3$ showed a weak single peak at 1,575 cm^{-1} and therefore $Co(MeAA)_2$ was not formed in these catalysts.

Fig. 6 shows FTIR spectra of NO adsorbed on Mo(c) and three Co-promoted catalysts with the same Co contents: Co(d)Mo(c), Co(d)Mo(c)_2M and Co(M)Mo(c). Peak I observed at 1,850 cm^{-1} was due to NO adsorbed on sulfided Co, including CoMoS and CoS_x, and peak III at 1,695 cm^{-1} was due to NO adsorbed on sulfided Mo. Peak II at 1,790 cm^{-1} originated from NO adsorbed on both sulfided Co and Mo [21-23]. The intensities of three peaks were normalized with respect to peak II. The intensity of peak III was lower for Co-promoted catalysts than for Mo(c) because the Mo surface was covered with added Co in the former catalysts. Among three Co-

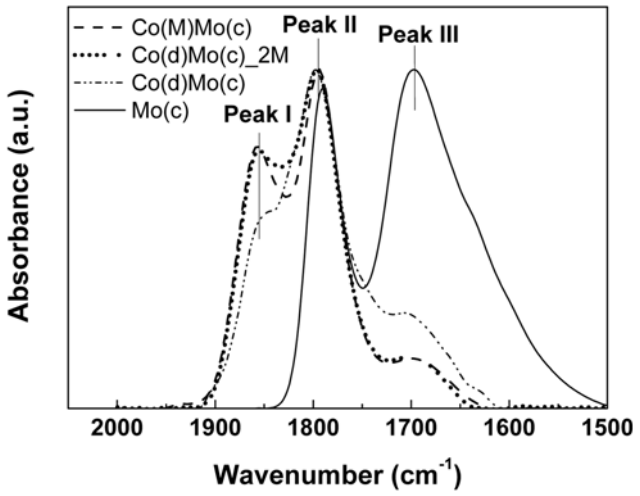

Fig. 6. FT-IR absorbance spectra of NO adsorbed on various Co MoS/Al_2O_3 catalysts. Sample notations are described in section 2.1.

promoted catalysts, Co(M)Mo(c) and Co(d)Mo(c)_2M showed a lower intensity of peak III than in the case of Co(d)Mo(c), indicating that Mo was covered with Co to a greater extent in the former catalysts. It is noteworthy that the IR spectra nearly overlapped for Co(d)Mo(c)_2M and Co(M)Mo(c).

The difference in the coverage of Mo with Co also affected the sulfidation of Co in the catalysts. That is, the relative intensity of peak I compared with the intensity of Peak III was higher for Co(M)Mo(c) and Co(d)Mo(c)_2M than for Co(d)Mo(c), i.e., Co(M)Mo(c)~Co(d)Mo(c)_2M>Co(d)Mo(c), which indicated that the Co species were sulfided to greater extents in the former two catalysts. Accordingly, catalysts prepared using MeAA as a chelating agent or $Co(MeAA)_2 \cdot 2H_2O$ as a Co precursor are expected to have larger amounts of the HDS-active CoMoS phase after sulfidation. It is also noteworthy that Co(M)Mo(c) and Co(d)Mo(c)_2M showed nearly identical surface properties prior to sulfidation, as analyzed by the above IR observations (Fig. 5).

3. TPS and TPR

Fig. 7 shows TPS of Co(d), either containing MeAA or not, and Mo(c). A small positive peak appearing at 310-320 K (Peak I) on Co(d)_M originated from the desorption of H_2S physically adsorbed on the sample [24,25]. Mo(c), which was expected to contain MoO_3 after the final calcination step, showed a large negative peak at 315-450 K (Peak II) because H_2S was consumed during the transformation of MoO_3 into Mo oxy-sulfides ($MoO_{3-x}S_x$) or MoS_3. The negative peak was followed by a sharp positive peak appearing at higher temperatures (Peak III), 450-500 K, which was due to the evolution of H_2S during the reduction of $MoO_{3-x}S_x$ or MoS_3 to $MoO_{3-x}S_{x-y}$ or MoS_2. The $MoO_{3-x}S_{x-y}$ species in Mo(c) were eventually converted to MoS_2 at higher temperatures, above 500 K (Peak IV) [26,27].

Co(d) showed a TPS result somewhat similar to that of Mo(c), except that Peaks II and III were shifted to higher temperatures, by about 50 K, from those of Mo(c). However, Peak III observed at 450-500 K for Co(d) was not due to the sulfidation of Co(d) but to the hydrogenation of elemental sulfur that had been produced by the reaction of $Co(NO_3)_2$ with H_2S [28]. Accordingly, the sulfidation of Co(d) was completed at *ca.* 450 K (Peak II), which was lower than temperature required for the complete sulfidation of Mo(c) to MoS_2, i.e., above 500 K (Peak IV).

Unlike the above two samples, Co(d)_M did not show a sharp positive Peak III at 450-550 K. Furthermore, Peak II of Co(d)_M was shifted to significantly higher temperatures, by about 100 K from that of Mo(c) and by 60 K from that of Co(d). The above results suggest that the Co species in Co(d) was stabilized by added MeAA.

The TPR patterns of three sulfided catalysts, Mo(c), Co(d)Mo(c) and Co(d)Mo(c)_2M, showed two negative peaks (Fig. 8). Peak I, observed at 400-500 K, was ascribed to the reduction of the S_x species chemisorbed at the edges of MoS_2 crystallites, which was related to the HDS activity. For example, Li et al. reported that the catalytic activity increased with a decrease in the peak temperature [29,30]. Peak II at 600-750 K, which was assigned to the reduction of catalytically inactive Co_9S_8 phase [29-32], was observed only for Co(d)

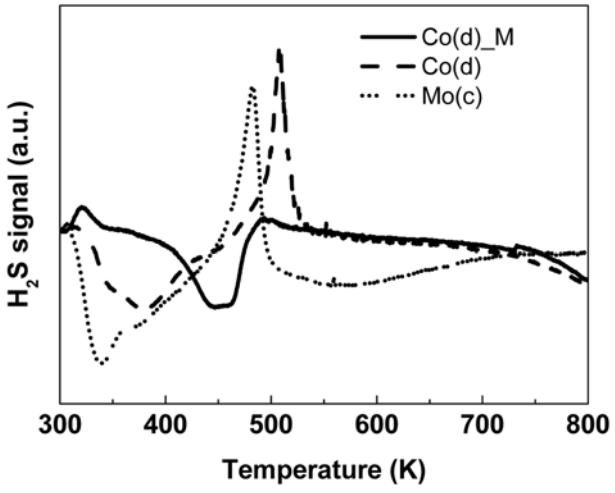

Fig. 7. Temperature-programmed sulfidation (TPS) of various samples. Sample notations are described in section 2.1. Mass signal representing H_2S (m/e=34) was measured.

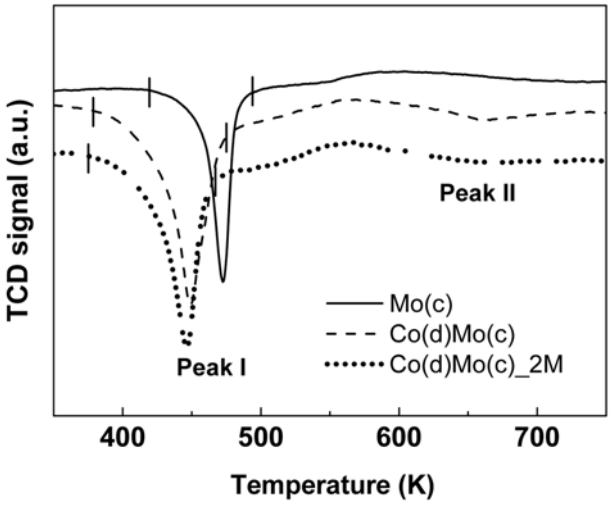

Fig. 8. Temperature-programmed reduction (TPR) of sulfide catalysts. Sample notations are described in section 2.1.

Mo(c) and Co(d)Mo(c)_2M.

Peak I, which was observed at 475 K for Mo(c), was shifted to 450 K for Co(d)Mo(c) and further to 445 K for Co(d)Mo(c)_2M. Accordingly, it can be concluded that the reactivity of the S_x species located at the edges of MoS_2 slabs was enhanced by Co promotion and to a greater extent by the addition of MeAA. The intensity of Peak II was lower for Co(d)Mo(c)_2M than for Co(d)Mo(c), indicating that the amount of inactive Co_9S_8 in the catalyst was decreased by the addition of MeAA.

DISCUSSIONS

1. Co(M)Mo(c) Prepared from $Co(MeAA)_2 \cdot 2H_2O$

Fig. 1 demonstrates that Co(M)Mo(c), prepared using $Co(MeAA)_2 \cdot 2H_2O$ as a new Co precursor, was more active than catalysts prepared from $Co(NO_3)_2 \cdot 6H_2O$ and using EDTA as a chelating agent. The improved activity of Co(M)Mo(c) originated from two factors. One was the high dispersion of MoS_2 crystallites, as indicated by HRTEM images (Fig. 4) showing the shortest average length of MoS_2 slabs (Table 2) for Co(M)Mo(c).

The other factor was that Co-Mo interactions were greater when $Co(MeAA)_2 \cdot 2H_2O$, instead of $Co(NO_3)_2 \cdot 6H_2O$, was used as a Co precursor. IR observations of NO adsorbed on sulfided catalysts (Fig. 6) indicated that the Mo surface was covered with Co to a greater extent in Co(M)Mo(c) and Co(d)Mo(c)_2M than in Co(d)Mo(c), obviously because Co-Mo interactions were stronger in the former catalysts. Accordingly, the HDS-active CoMoS phase was produced in larger amounts in the former catalysts than in Co(d)Mo(c).

2. Formation of *In Situ* $Co(MeAA)_2 \cdot 2H_2O$

Although $Co(MeAA)_2 \cdot 2H_2O$ was better than $Co(NO_3)_2 \cdot 6H_2O$ as a Co precursor for preparing highly active HDS catalysts, there were a few limitations to its industrial application. One was an economic disadvantage due to the high price of $Co(MeAA)_2 \cdot 2H_2O$. The others were that NaOH and methanol were required for the synthesis of $Co(MeAA)_2 \cdot 2H_2O$ and an organic solvent, 1,4-dioxane, for dissolving the water-insoluble Co precursor. Accordingly, we attempted to synthesize the Co precursor *in-situ* on the catalyst surface simply by adding an aqueous solution of MeAA to the catalyst, without using NaOH, methanol or an organic solvent.

IR results in Fig. 5 indicated that the surface functional groups of Co(d)Mo(c) became similar to those of $Co(MeAA)_2 \cdot 2H_2O$ when increased amounts of MeAA were added to the conventional catalyst. The HDS activity of Co(d)Mo(c)_xM approached that of Co(M)Mo(c) with an increase in the amounts of added MeAA (Fig. 2), suggesting that $Co(NO_3)_2$ in Co(d)Mo(c) was converted to a compound similar to $Co(MeAA)_2$ by reaction with added MeAA. The $Co(MeAA)_2$ compound formed by *in-situ* synthesis promoted the dispersion of MoS_2 slabs and the formation of CoMoS phase, eventually to increase the overall activity and the relative rates of DDS over HYD in HDS (Fig. 3).

However, the beneficial effect of MeAA on the catalytic activity was not observed when MeAA was added to Co(c)Mo(c), which was finally calcined in air after impregnation with $Co(NO_3)_2 \cdot 6H_2O$ (Table 1). The reaction results were in accordance with IR observations (Fig. 5), which indicated that the surface groups characteristic to $Co(MeAA)_2 \cdot 2H_2O$ were not observed in Co(c)Mo(c)_2M. Accordingly, the *in-situ* synthesis of $Co(MeAA)_2$ compound proceeded only when added MeAA reacted with the surface $Co(NO_3)_2$ species that remained in Co(d)Mo(c). In the case of Co(c)Mo(c), the Co species were largely in CoO_x, which did not react with MeAA.

TPS observations (Fig. 7) indicated that Co(d) was sulfided at higher temperatures when MeAA was added to it, which agreed with previous reports that chelating agents delayed the sulfidation of Co eventually to suppress the formation of bulk Co sulfides and to promote the formation of the active CoMoS phase [9-13]. It is noteworthy that Co(d)_M was sulfided at temperatures, 400-500 K, lower than those for Co-EDTA, which proceeded at above 650 K. The excessive stability of the Co-EDTA complex allowed the sulfidation of Co at high temperatures and eventually the growth of MoS_2 slabs, which was detrimental to the catalytic activity [14,15]. HRTEM results in this study (Fig. 4) indicated that the average length of MoS_2 slabs decreased in an order, Co(d)Mo(c)>Co(E)Mo(c)>>Co(M)Mo(c), which was in accordance with the activity results. The reactivity of the S species located at the edges of MoS_2 crystallites, represented by TPR (Fig. 8), was higher in Co(d)Mo(c)_2M than in Co(d)Mo(c), again in accordance with the activity results.

CONCLUSIONS

The HDS activity of $CoMoS/Al_2O_3$ was improved when the catalyst was prepared using $Co(MeAA)_2 \cdot 2H_2O$, instead of $Co(NO_3)_2 \cdot 6H_2O$, as a Co precursor. The former precursor was more stable than the latter under sulfidation condition, which delayed the sulfidation of Co and eventually promoted the formation of the HDS-active CoMoS phase. Catalysts of similar activity could be obtained simply by impregnating conventional catalysts, prepared using $Co(NO_3)_2 \cdot 6H_2O$ and finally dried in air at 393 K, with an aqueous solution of MeAA. IR observations of the MeAA-added catalysts indicated that the *in-situ* synthesis of $Co(MeAA)_2$ proceeded on the catalyst surface by reaction between Co and added MeAA. This method was advantageous over the method of directly adding $Co(MeAA)_2 \cdot 2H_2O$ to impregnation solution because the former method was cheaper and free from using a basic material and organic solvent, unlike the latter method.

ACKNOWLEDGEMENT

This work was supported by Brain Korea 21 Project (BK21) and SK Innovation Co., Ltd.

REFERENCES

1. C. Song and X. Ma, *Appl. Catal. B: Environ.*, **41**, 207 (2003).
2. S. Eijsbouts, A. A. Battiston and G. C. van Leerdam, *Catal. Today*, **130**, 361 (2008).
3. S. J. Moon and S. K. Ihm, *Korean J. Chem. Eng.*, **11**(2), 111 (1994).
4. H. Topsøe and B. S. Clausen, *Appl. Catal.*, **25**, 273 (1986).
5. K. L. Kim and K. S. Choi, *Korean J. Chem. Eng.*, **5**(2), 177 (1988).
6. Y. Okamoto and T. Kubota, *Catal. Today*, **86**, 31 (2003).
7. H. Topsøe, B. S. Clausen, R. Candia, C. Wivel and S. Mørup, *J. Catal.*, **68**, 433 (1981).
8. C. Wivel, R. Candia, B. S. Clausen, S Mørup and Henrik Topsøe, *J. Catal.*, **68**, 453 (1981).
9. A. J. van Dillen, R. J. A. M. Terörde, D. J. Lensveld, J. W. Geus and

K. P. de Jong, *J. Catal*., **216**, 257 (2003).
10. T. Kubota, N. Rinaldi, K. Okumura, T. Honma, S. Hirayama and Y. Okamoto, *Appl. Catal. A: Gen*., **373**, 214 (2010).
11. R. Cattaneo, F. Rota and R. Prins, *J. Catal*., **199**, 318 (2001).
12. R. Cattaneo, T. Shido and R. Prins, *J. Catal*., **185**, 199 (1999).
13. T. Shimizu, K. Hiroshima, T. Honma, T. Mochizuki and M. Yamada, *Catal. Today*, **45**, 271 (1998).
14. N. Frizi, P. Blanchard, E. Payen, P. Baranek, M. Rebeilleau, C. Dupuy and J. P. Dath, *Catal. Today*, **130**, 272 (2008).
15. S. L. González-Cortés, T. C. Xiao, P. M. F. J. Costa, B. Fontal and M. L. H. Green, *Appl. Catal. A: Gen*., **270**, 209 (2004).
16. D. S. Sankhla, R. C. Mathur and S. N. Misra, *J. Inor. Nucl. Chem*., **42**, 489 (1980).
17. M. A. Lélias, E. Le Guludec, L. Mariey, J. van Gestel, A. Travert, L. Oliviero and F. Maugé, *Catal. Today*, **150**, 179 (2010).
18. F. Bataille, J. L. Lemberton, P. Michaud, G. Pérot, M. Vrinat, M. Lemaire, E. Schulz, M. Breysse and S. Kasztelan, *J. Catal*., **191**, 409 (2000).
19. T. Kabe, A. Ishihara and Q. Zhang, *Appl. Catal. A: Gen*., **97**, L1 (1993).
20. V. Meille, E. Schulz, M. Lemaire and M. Vrinat, *J. Catal*., **170**, 29 (1997).
21. R. Nava, R. A. Ortega, G. Alonso, C. Ornelas, B. Pawelec and J. L. G. Fierro, *Catal. Today*, **127**, 70 (2007).
22. N. Y. Topsøe and H. Topsøe, *J. Catal*., **84**, 386 (1983).
23. M. S. Rana, J. Ramírez, A. Gutiérrez-Alejandre, J. Ancheyta, L. Cedeño and S. K. Maity, *J. Catal.*, **246**, 100 (2007).
24. P. Arnoldy, J. L. de Booys, B. Scheffer and J. A. Moulijn, *J. Catal*., **96**, 122 (1985).
25. K. Inamura, T. Takyu, Y. Okamoto, K. Nagata and T. Imanaka, *J. Catal*., **133**, 498 (1992).
26. M. de Boer, A. J. van Dillen, D. C. Koningsberger and J. W. Geus, *J. Phys. Chem*., **98**, 7862 (1994).
27. R. Iwamoto, K. Inamura, T. Nozaki and A. Iino, *Appl. Catal. A: Gen*., **163**, 217 (1997).
28. S. I. Lee, A. Cho, J. H. Koh, S. H. Oh and S. H. Moon, *Appl. Catal. B: Environ*., **101**, 220 (2011).
29. M. Li, H. Li, F. Jiang, Y. Chu and H. Nie, *Fuel*, **88**, 1281 (2009).
30. B. Scheffer, N. J. J. Dekker, P. J. Mangnus and J. A. Moulijn, *J. Catal*., **121**, 31 (1990).
31. P. J. Mangnus, A. Riezebos, A. D. Vanlangeveld and J. A. Moulijn, *J. Catal*., **151**, 178 (1995).
32. N. K. Nag, D. Fraenkel, J. A. Moulijn and B. C. Gates, *J. Catal*., **66**, 162 (1980).